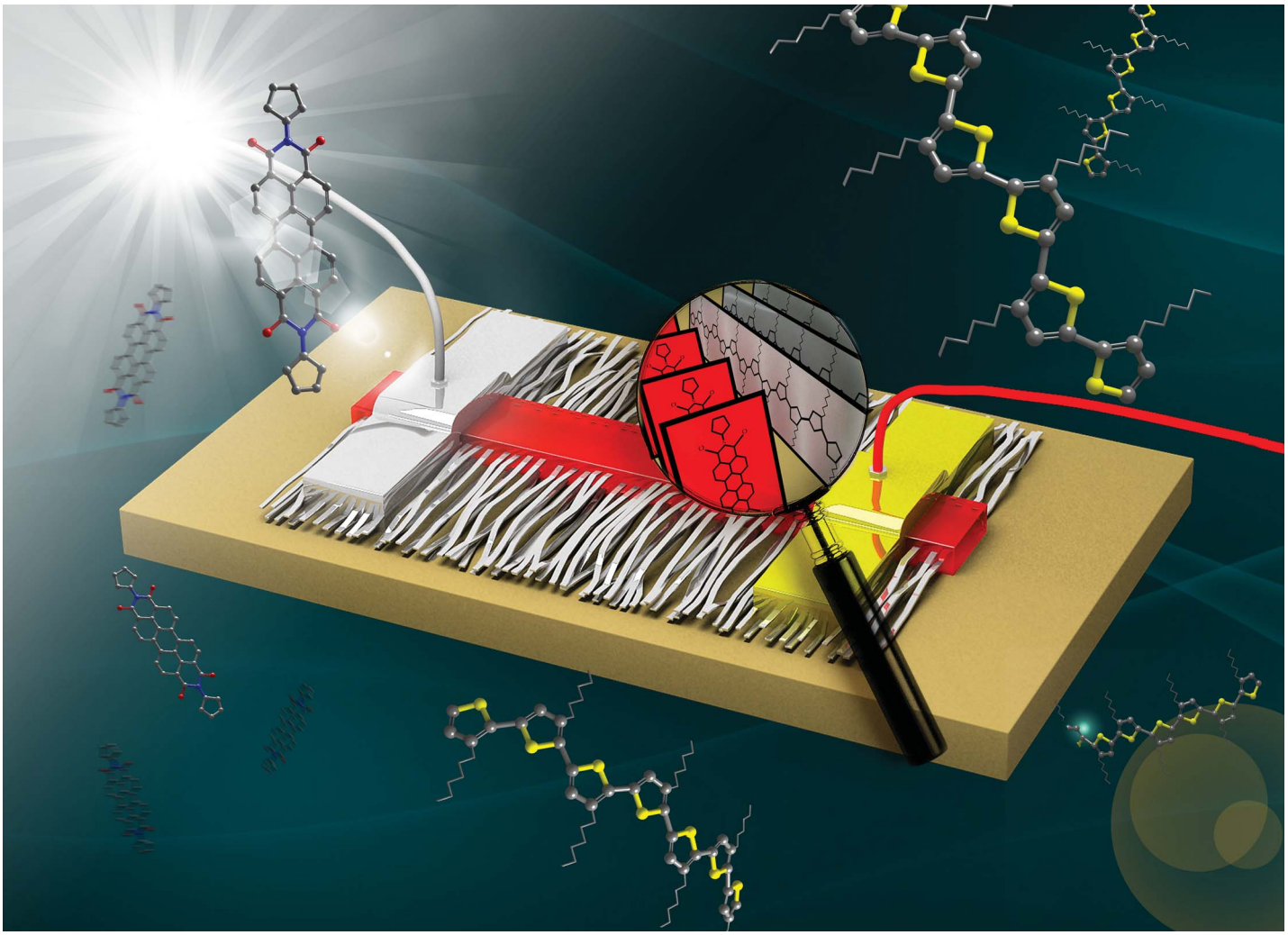

Highlighting research from the Laboratory of Prof. Ling Zang at the University of Utah

Title: Anomalous high photovoltages observed in shish kebab-like organic p–n junction nanostructures

Anomalous high photovoltages, significantly above the energy level offset between the LUMO of the acceptor and the HOMO of the donor, are observed in horizontal photovoltaic devices employing discrete shish kebab-like organic p–n junction nanostructures.

As featured in:

See L. Li *et al.*, *Polym. Chem.*, 2014, **5**, 309.

ROYAL SOCIETY OF CHEMISTRY

www.rsc.org/polymers

Registered charity number: 207890

Polymer Chemistry

COMMUNICATION

View Article Online
View Journal | View Issue

Anomalous high photovoltages observed in shish kebab-like organic p–n junction nanostructures†

Cite this: *Polym. Chem.*, 2014, **5**, 309

Received 30th July 2013
Accepted 28th August 2013

DOI: 10.1039/c3py01026k

www.rsc.org/polymers

Ligui Li,[ab] Daniel L. Jacobs,[a] Benjamin R. Bunes,[a] Helin Huang,[a] Xiaomei Yang[a] and Ling Zang*[a]

Published on 30 August 2013. Downloaded by University of Utah on 29/08/2017 22:49:00.

We report the observation of anomalous high photovoltages, which are significantly higher than the energy level offset between the highest occupied molecular orbital (HOMO) of the electron donor (D) and the lowest unoccupied molecular orbital (LUMO) of the acceptor (A), in single trunk shish kebab-like organic p–n junction nanostructures. Creation of such high photovoltages is likely due to the special intermolecular orientation in the unique structure.

Semiconductor p–n junction nanowires have attracted particular attention during the past decades not only because they can serve as ideal model systems in fundamental research, but also because they offer opportunities in practical applications, for instance in photovoltaic (PV) devices.[1–5] In contrast to the well-developed inorganic p–n junction nanowires, only a few organic or hybrid organic–inorganic p–n junction nanostructures have been reported to date due to difficulties in finding appropriate complementary D and A materials for preparing p–n nanojunctions under mild conditions.[6–10]

Recently, several interesting shish kebab-like organic p–n heterojunction structures have been reported.[11,12] Such branching nanostructures provide a high density of D–A junctions and thereby are expected to produce efficient exciton dissociation, as observed in bulk-heterojunction (BHJ) solar cells. Moreover, compared to the random distribution of D–A components in BHJ systems, the well-oriented molecular arrangement in the shish kebab structures will also enable directional control of charge migration, which in turn may help us to design and build a new type of PV device to study the molecule-structure–function relationship in organic semiconductor materials. However, to the best of our knowledge, no PV property/application of these shish kebab-like structures has been reported as yet. In the present work, we report the fabrication of well-defined shish kebab-like nanostructures from a robust A molecule and a semiconducting polymer (acting as D), and the construction of a horizontal PV device using a single shish kebab structure. Remarkably, the device demonstrated anomalous high photovoltages, much higher than the upper limit determined by the energy level offset between the HOMO of D and the LUMO of A. This finding may open up a new way to increase the V_{oc} of organic PV devices without resorting to the series tandem device architecture, which usually needs complicated and sophisticated fabrication technology.[13–16]

The materials used in this study were highly regioregular poly(3-hexylthiophene) (P3HT) as the donor and *N*,*N*-(dicyclopentyl) perylene-3,4,9,10-tetracarboxylic diimide (C5-PTCDI) as the acceptor (Fig. 1a). The PTCDI derivatives form a robust class of materials with high thermal and photo-stability.[17] The strong electron affinity and extensive absorption in the visible light region make PTCDI a suitable A material for organic solar cells. Moreover, the rigid, planar geometry of PTCDI favors one-dimensional self-assembly into elongated fibril structures, along which the extended π–π stacking interaction enables efficient charge transport through π-electron delocalization.[18,19]

Fig. 2a shows a nanobelt structure prepared from C5-PTCDI through slow evaporation of a dilute chloroform solution (0.3 mg mL^{-1}). Several selected area electron diffraction (SAED)

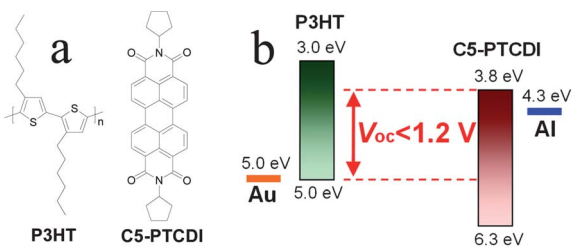

Fig. 1 (a) Molecular structures of regioregular P3HT and C5-PTCDI. (b) Energy level offset showing the upper limit of V_{oc} in PV devices based on a single C5-PTCDI/P3HT junction.

[a]*Department of Materials Science and Engineering, University of Utah, Salt Lake City, Utah 84112, USA. E-mail: lzang@eng.utah.edu; Fax: +1-801-585-0625; Tel: +1-801-587-1551*

[b]*School of Environment and Energy, South China University of Technology, Guangzhou 510006, P. R. China*

† Electronic supplementary information (ESI) available: SAED images, AFM image, SEM images and *I–V* plots. See DOI: 10.1039/c3py01026k

Published on 30 August 2013. Downloaded by University of Utah on 29/08/2017 22:49:00.

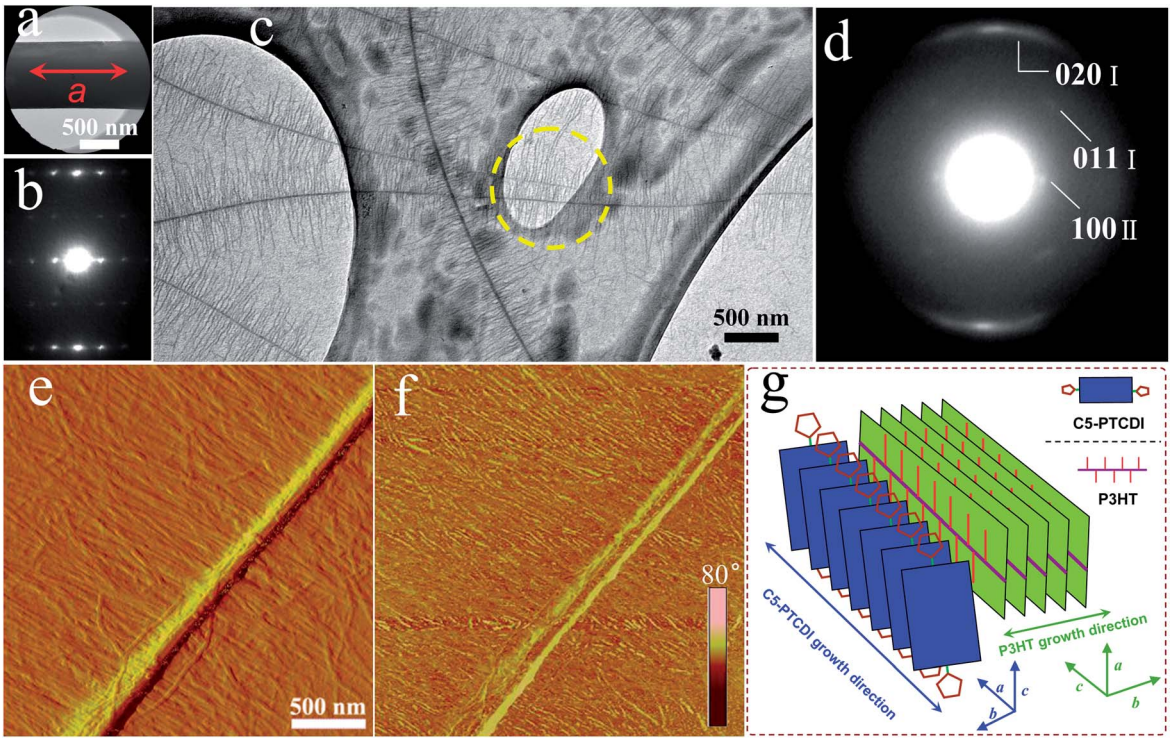

Fig. 2 (a) Bright field TEM (BF-TEM) image of a C5-PTCDI single-crystalline nanobelt and (b) its corresponding SAED pattern. (c) BF-TEM image of C5-PTCDI/P3HT shish kebab-like structures and (d) a SAED pattern from the area enclosed by the yellow, dashed circle in (c); the diffraction indices of P3HT are indicated as group I, while the diffraction index of C5-PTCDI is indicated as group II. AFM (e) amplitude and its corresponding phase (f) image showing the distribution of P3HT nanofibers in a typical C5-PTCDI/P3HT shish kebab-like structure; the corresponding topography image is shown in Fig. S2.† (g) Schematic illustration of the intermolecular orientation of P3HT and C5-PTCDI in shish kebab-like structures.

images taken at different spots of the nanobelt show the same diffraction geometry (Fig. S1†), indicating the single crystalline nature throughout the nanobelt. A representative SAED pattern taken from the nanobelt is shown in Fig. 2b. This diffraction pattern corresponds to a single-crystalline phase with lattice constants of $a = 10.57$ Å, $b = 5.96$ Å, and $\gamma = 88.9°$, which is close to the lattice constants of a similar PTCDI reported by others.[20] By comparing the obtained SAED pattern with its corresponding bright-field TEM image (Fig. 2a), we find that the preferred growth direction of C5-PTCDI is parallel to its crystallographic *a* axis, along which the C5-PTCDI molecules show slipped π–π stacking (Fig. 2g).[17,21]

When C5-PTCDI nanobelts were added to P3HT/xylene solution during the crystallization process of P3HT, shish kebab-like structures were obtained (Fig. 2c), with P3HT nanofibers branching off the PTCDI trunk normal to its axis. The diameter of P3HT nanofibers was measured to be *ca.* 20 nm, consistent with the sizes typically reported.[22–24] Fig. 2d shows a SAED pattern recorded on the location marked by the yellow dashed circle in Fig. 2c. By using the previously reported lattice constants of P3HT,[25,26] *i.e.* $a = 16.6$ Å, $b = 7.8$ Å, $c = 8.36$ Å, $\alpha = \beta = \gamma = 90°$, the outer two bright arcs with a *d*-spacing of 3.9 Å are indexed to the (020) plane of P3HT, while the four short diffused arcs with a *d*-spacing of 5.32 Å are assigned to the reflection of the crystallographic (011) plane and its symmetric planes of P3HT. The *d*-spacing of the two diffused spots near the central beam is 10.33 Å, which matches the aforementioned lattice constant of *a* in the C5-PTCDI single crystal, implying that they can be indexed to the (100) plane of C5-PTCDI. When comparing this indexed diffraction pattern with the corresponding selected area in Fig. 2c, we found that the distribution of diffraction spots and arcs in the SAED pattern is consistent with the relative orientation of C5-PTCDI and P3HT in the TEM image. These observations confirm that the central trunk of the shish-kebab structure is composed of C5-PTCDI single crystals while the branches are composed of P3HT nanofibers.

To get deeper insight into the intermolecular orientation of P3HT and C5-PTCDI in the structure, atomic force microscopy (AFM) characterization was also performed. As shown in Fig. 2e, dense P3HT nanofibers only grow from the edges of the belt-shaped C5-PTCDI crystals, with one end connecting to the core. In the AFM phase image (Fig. 2f), it distinctly shows that the phase of the top surface of the C5-PTCDI crystal is different from those of P3HT nanofibers and both edges of C5-PTCDI itself, which further confirms that the P3HT nanofibers only grow from the edges. We speculate that the C5-PTCDI crystal may serve as a nucleus for P3HT to crystallize on its edge surface. Accordingly, the intermolecular orientation of P3HT and C5-PTCDI in the shish kebab-like structures can be approximately sketched as that in Fig. 2g.

Remarkably these shish kebab-like structures demonstrated unprecedentedly high photovoltages. To our knowledge, there

 This journal is © The Royal Society of Chemistry 2014

Published on 30 August 2013. Downloaded by University of Utah on 29/08/2017 22:49:00.

is much less work reported on the enhancement of V_{oc} compared to other factors such as short circuit current density (J_{sc}) and filling factor (FF). The difficulty of increasing V_{oc} is mainly due to the fact that it is generally an intrinsic property of the D and A materials. The theoretical upper limit of V_{oc} in OPV devices is normally determined by the energy level offset between the HOMO level of the D material and the LUMO level of the A material.[27–32] Delicate optimization of the energy level offset often results in only a slight increase in V_{oc}. As indicated in Fig. 1b, the bandgap of P3HT is *ca.* 2.0 eV,[13] and the energy level offset between the HOMO of P3HT and the LUMO of C5-PTCDI is *ca.* 1.2 eV. Therefore, the V_{oc} is expected to be lower than 1.2 V in a single-junction device.

To study the PV properties of the shish kebab-like structures, aluminum (Al) and gold (Au) contacts were thermally evaporated onto the structures as shown schematically in Fig. 3a. Because P3HT nanowires only grow on the edges of C5-PTCDI crystals, top deposited electrodes can be in direct contact both P3HT and C5-PTCDI without resorting to the rigorous preparation conditions and treatments usually applied in inorganic nanowire processing.[1,15,33,34] In the dark, the devices employing the architecture illustrated in the left part of Fig. 3a show rectifying properties in the corresponding *I–V* curves (Fig. S3†), which indicate that such devices are typical diodes. Under simulated AM1.5G light illumination, a representative device with a V_{oc} of 2.3 V is shown in the right part of Fig. 3a. Though the values obtained in such devices exhibit a distribution of 1.6–2.5 V, all are significantly larger than the theoretical upper limit of V_{oc} in a single-junction device (Fig. 1b). The plot in Fig. 3a yields a J_{sc} of 0.0297 mA cm^{-2}, a FF of 0.31, and a power conversion efficiency (PCE) of 0.0528%. It is worth noting that the PCE of this unique shish kebab-like p–n junction is nearly 8 times and 1.5 times higher than the previously reported organic single p–n junction[8] and hybrid coaxial[10] nanowire

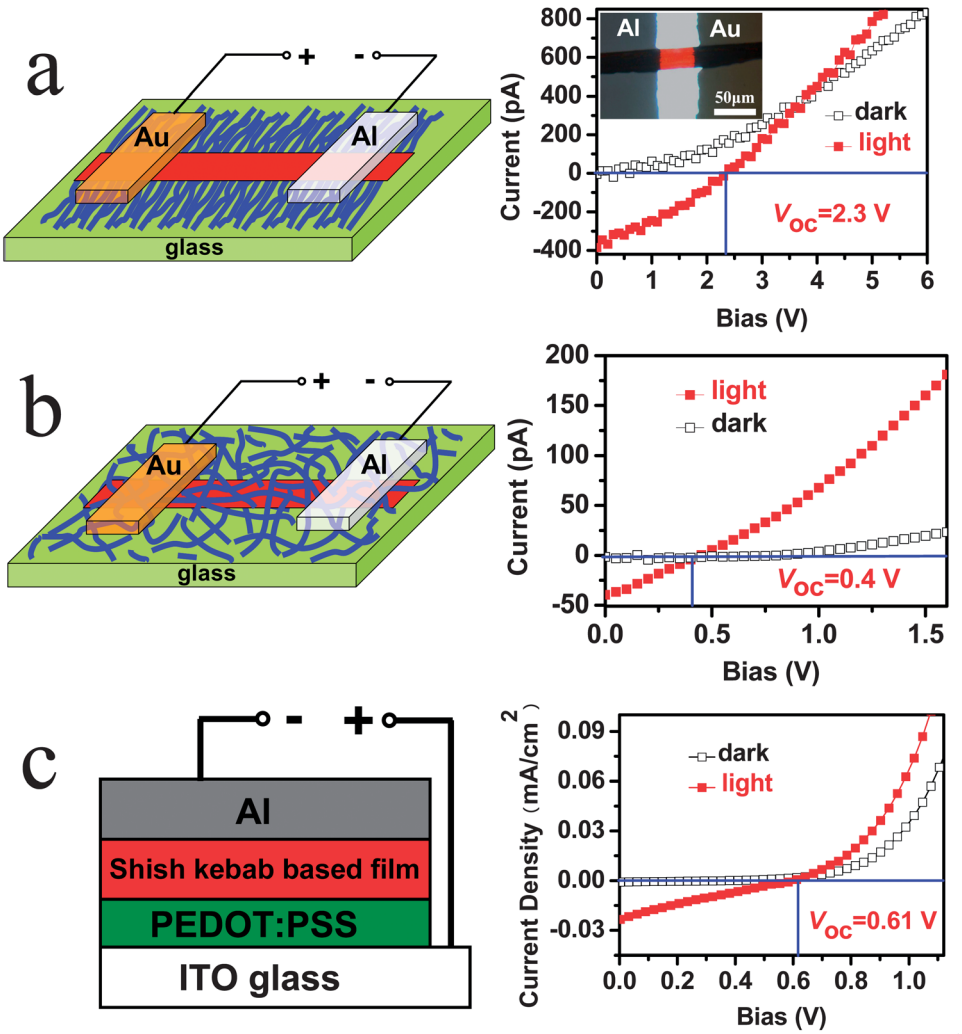

Fig. 3 Device architectures and the corresponding *I–V* characteristics measured under dark and simulated AM1.5G light illumination from a glass substrate bottom at 40 mW cm^{-2}. (a) PV device employing a discrete C5-PTCDI/P3HT shish kebab-like structure; the inset shows the optical microscopic image of the device. (b) PV device based on a C5-PTCDI single crystal covered by random P3HT fibers. (c) Solar cell employing the traditional sandwich structure with C5-PTCDI/P3HT shish kebab-like structures as the photoactive layer, with a film thickness of *ca.* 140 nm. Electrode gap in (a) and (b) is 40 μm.

Published on 30 August 2013. Downloaded by University of Utah on 29/08/2017 22:49:00.

based PV devices, respectively, while the relatively low J_{sc} is likely due to the much longer charge transport path. We expect to increase the J_{sc} and PCE by reducing the electrode gap distance so that charge recombination can be substantially reduced in future. Scanning electron microscopy (SEM) imaging of a working device (Fig. S4†) shows that the edge surfaces of the C5-PTCDI crystal are densely covered by perpendicularly oriented P3HT nanofibers, confirming that the photoactive part of this device is a shish kebab-like structure and this structure remains nondestructive during the device fabrication. Further increasing the gap distance to 80 μm did not contribute to an increase of the V_{oc} and J_{sc} (Fig. S5†).

To preliminarily study the origin of the high photovoltage observed, two reference devices were fabricated, shown schematically in Fig. 3b and c. When the C5-PTCDI crystalline fiber is covered by random P3HT nanofibers *via* spin casting preformed P3HT nanofibers onto the C5-PTCDI crystal, the corresponding device showed a V_{oc} of only 0.4 V (Fig. 3b). Similarly, when the C5-PTCDI/P3HT shish kebab nanostructures were sandwiched between Al and ITO electrodes as a BHJ solar cell, the device demonstrated a V_{oc} of only 0.61 V (Fig. 3c). These observations explicitly indicate that the high V_{oc} observed in Fig. 3a is highly correlated with the special shish kebab-like morphology and the device architecture.

Although not yet completely understood, we speculate that the high V_{oc} obtained within our devices may be ascribed to the presence of a large amount of charge carriers (benefiting from the high density of p–n junctions for efficient exciton dissociation and extended directional charge transport) at the interfaces between P3HT nanofibers and the C5-PTCDI central trunk, a phenomenon somewhat similar to what was observed in horizontal inorganic solar cells.[35,36] Indirect support for this assumption is the different dependence of V_{oc} on light intensity.

As shown in Fig. 4, the V_{oc} of the shish kebab-based device dramatically increased with light intensity, and reached a plateau when the light intensity increased above 40 mW cm^{-2}. In contrast, the BHJ based device only showed a slight increase of V_{oc} even at high light intensities. For the device with randomly distributed P3HT nanofibers on C5-PTCDI, the V_{oc} remained nearly unchanged with increasing light intensity. In general, V_{oc} increases with light intensity due to the presence of a large amount of charge carriers, but the increase is usually very small (~100 mV), even with over two orders of magnitude increase in light intensity.[37–41] Therefore, the large dependence of V_{oc} on light intensity in the low intensity region observed for the shish-kebab based device implies the presence of a large amount of charges across the D and A interface. As a result, the electric potential built up by the large numbers of charges will dominate the intrinsic V_{oc}, making the V_{oc} structure dependent and no longer material dependent (Fig. S10†). More systematic work is still ongoing to thoroughly study the structure–function relationship in these shish-kebab like p–n junction nanostructures.

In summary, the presence of C5-PTCDI single crystals in the solution where P3HT crystallizes will facilitate the formation of shish kebab-like nanostructures, with the central C5-PTCDI elongated crystal as shish and the perpendicularly branching P3HT nanowires on both sides of it as kebabs. Such unique shish-kebab like p–n junction nanostructures not only exhibit photocurrent rectification, but also anomalous high V_{oc}, which is higher than the energy level offset between the LUMO of A and the HOMO of D. Stronger light intensity dependence of thus obtained V_{oc} compared to other reference devices indicates that the origin of such unprecedented high V_{oc} may be due to the presence of large numbers of charge carriers across the interface between P3HT and C5-PTCDI. These findings may enable a new way to realize high photovoltage in organic single-wire based solar cells, and the unique shish kebab-like structures provide a new platform to study the PV behaviors in organic semiconductors.

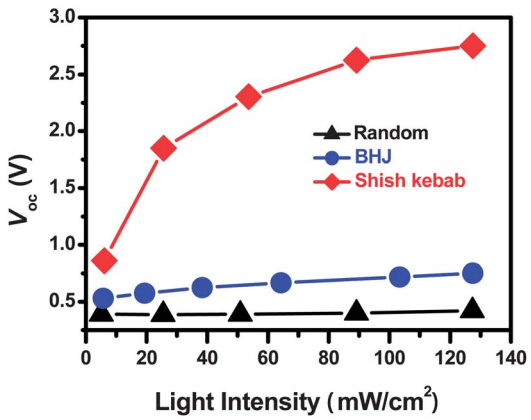

Fig. 4 The light intensity dependence of V_{oc}. The three devices shown in Fig. 3a–c (namely shish kebab, random and BHJ, respectively) were tested under the same conditions as employed in Fig. 3, but with varying light intensity.

Acknowledgements

We thank the National Science Foundation for support through CAREER (#CHE 0931466), IGERT (#DGE-0903715) and MRSEC Project (#1121252). We are also grateful to the support from the USTAR program of the State of Utah. We thank Prof. Zeev Valy Vardeny for his helpful discussion.

Notes and references

1 B. Tian, X. Zheng, T. J. Kempa, Y. Fang, N. Yu, G. Yu, J. Huang and C. M. Lieber, *Nature*, 2007, **449**, 885.
2 C. Gutsche, R. Niepelt, M. Gnauck, A. Lysov, W. Prost, C. Ronning and F.-J. Tegude, *Nano Lett.*, 2012, **12**, 1453.
3 A. I. Hochbaum and P. Yang, *Chem. Rev.*, 2012, **110**, 527.
4 Z. Jiang, Q. Qing, P. Xie, R. Gao and C. M. Lieber, *Nano Lett.*, 2012, **12**, 1711.
5 R. He, T. D. Day, M. Krishnamurthi, J. R. Sparks, P. J. A. Sazio, V. Gopalan and J. V. Badding, *Adv. Mater.*, 2013, **25**, 1461.
6 Y. Guo, Q. Tang, H. Liu, Y. Zhang, Y. Li, W. Hu, S. Wang and D. Zhu, *J. Am. Chem. Soc.*, 2008, **130**, 9198.
7 C. M. Rodd and R. Agarwal, *Nano Lett.*, 2011, **11**, 3460.

 This journal is © The Royal Society of Chemistry 2014

Published on 30 August 2013. Downloaded by University of Utah on 29/08/2017 22:49:00.

8 Y. Zhang, H. Dong, Q. Tang, S. Ferdous, F. Liu, S. C. B. Mannsfeld, W. Hu and A. L. Briseno, *J. Am. Chem. Soc.*, 2010, **132**, 11580.
9 Q. H. Cui, L. Jiang, C. Zhang, Y. S. Zhao, W. Hu and J. Yao, *Adv. Mater.*, 2012, **24**, 2332.
10 A. L. Briseno, T. W. Holcombe, A. I. Boukai, E. C. Garnett, S. W. Shelton, J. J. M. Fréchet and P. Yang, *Nano Lett.*, 2010, **10**, 334.
11 J. Liu, J. Zou and L. Zhai, *Macromol. Rapid Commun.*, 2009, **30**, 1387.
12 L. Bu, E. Pentzer, F. A. Bokel, T. Emrick and R. C. Hayward, *ACS Nano*, 2012, **6**, 10924.
13 J. Y. Kim, K. Lee, N. E. Coates, D. Moses, T.-Q. Nguyen, M. Dante and A. J. Heeger, *Science*, 2007, **317**, 222.
14 L. Yang, S. Wang, Q. Zeng, Z. Zhang, T. Pei, Y. Li and L.-M. Peng, *Nat. Photonics*, 2011, **5**, 672.
15 T. J. Kempa, B. Tian, D. R. Kim, J. Hu, X. Zheng and C. M. Lieber, *Nano Lett.*, 2008, **8**, 3456.
16 M. Heurlin, P. Wickert, S. Fält, M. T. Borgström, K. Deppert, L. Samuelson and M. H. Magnusson, *Nano Lett.*, 2011, **11**, 2028.
17 L. Zang, Y. Che and J. S. Moore, *Acc. Chem. Res.*, 2008, **41**, 1596.
18 Y. Che, A. Datar, K. Balakrishnan and L. Zang, *J. Am. Chem. Soc.*, 2007, **129**, 7234.
19 Y. Che, H. Huang, M. Xu, C. Zhang, B. R. Bunes, X. Yang and L. Zang, *J. Am. Chem. Soc.*, 2011, **133**, 1087.
20 J. H. Oh, H. W. Lee, S. Mannsfeld, R. M. Stoltenberg, E. Jung, Y. W. Jin, J. M. Kim, J.-B. Yoo and Z. Bao, *Proc. Natl. Acad. Sci.U. S. A.*, 2009, **106**, 6065.
21 Y. Che, X. Yang, K. Balakrishnan, J. Zuo and L. Zang, *Chem. Mater.*, 2009, **21**, 2930.
22 K. J. Ihn, J. Moulton and P. Smith, *J. Polym. Sci., Part B: Polym. Phys.*, 1993, **31**, 735.
23 L. G. Li, G. H. Lu and X. N. Yang, *J. Mater. Chem.*, 2008, **18**, 1984.
24 Y. Guo, L. Jiang, X. Ma, W. Hu and Z. Su, *Polym. Chem.*, 2013, **4**, 4308.
25 K. Tashiro, M. Kobayashi, T. Kawai and K. Yoshino, *Polymer*, 1997, **38**, 2867.
26 D. H. Kim, J. T. Han, Y. D. Park, Y. Jang, J. H. Cho, M. Hwang and K. Cho, *Adv. Mater.*, 2006, **18**, 719.
27 E. Kymakis, I. Alexandrou and G. A. J. Amaratunga, *J. Appl. Phys.*, 2003, **93**, 1764.
28 M. C. Scharber, D. Mühlbacher, M. Koppe, P. Denk, C. Waldauf, A. J. Heeger and C. J. Brabec, *Adv. Mater.*, 2006, **18**, 789.
29 B. P. Rand, D. P. Burk and S. R. Forrest, *Phys. Rev. B: Condens. Matter Mater. Phys.*, 2007, **75**, 115327.
30 A. Gadisa, M. Svensson, M. R. Andersson and O. Inganäs, *Appl. Phys. Lett.*, 2004, **84**, 1609.
31 K. Vandewal, K. Tvingstedt, A. Gadisa, O. Inganäs and J. V. Manca, *Nat. Mater.*, 2009, **8**, 904.
32 K. L. Mutolo, E. I. Mayo, B. P. Rand, S. R. Forrest and M. E. Thompson, *J. Am. Chem. Soc.*, 2006, **128**, 8108.
33 Y. Wu, R. Fan and P. Yang, *Nano Lett.*, 2002, **2**, 83.
34 M. S. Gudiksen, L. J. Lauhon, J. Wang, D. C. Smith and C. M. Lieber, *Nature*, 2002, **415**, 617.
35 H. Levi Aharoni, D. Azulay, O. Millo and I. Balberg, *Appl. Phys. Lett.*, 2008, **92**, 112109.
36 S. Y. Yang, J. Seidel, S. J. Byrnes, P. Shafer, C.-H. Yang, M. D. Rossell, P. Yu, Y.-H. Chu, J. F. Scott, J. W. Ager III, L. W. Martin and R. Ramesh, *Nat. Nanotechnol.*, 2010, **5**, 143.
37 J. Albero, Y. Zhou, M. Eck, F. Rauscher, P. Niyamakom, I. Dumsch, S. Allard, U. Scherf, M. Krüger and E. Palomares, *Chem. Sci.*, 2011, **2**, 2396.
38 S. Ryuzaki and J. Onoe, *J. Phys. D: Appl. Phys.*, 2011, **44**, 265102.
39 L. J. A. Koster, V. D. Mihailetchi, R. Ramaker and P. W. M. Blom, *Appl. Phys. Lett.*, 2005, **86**, 123509.
40 M. M. Mandoc, F. B. Kooistra, J. C. Hummelen, B. d. Boer and P. W. M. Blom, *Appl. Phys. Lett.*, 2007, **91**, 263505.
41 D. Credgington, Y. Kim, J. Labram, T. D. Anthopoulos and J. Durrant, *J. Phys. Chem. Lett.*, 2011, **2**, 2759.